ACS OMEGA

Open Access

http://pubs.acs.org/journal/acsodf

Article

Heterocyclic Donor Moiety Effect on Optical Nonlinearity Behavior of Chrysene-Based Chromophores with Push−Pull Configuration *via* the Quantum Chemical Approach

Faiz Rasool,*,# Gang Wu, Iqra Shafiq,# Shehla Kousar, Saba Abid, Norah Alhokbany, and Ke Chen*

Cite This: *ACS Omega* 2024, 9, 3596−3608

Read Online

ACCESS | Metrics & More | Article Recommendations | Supporting Information

ABSTRACT: Organic-based nonlinear optical (NLO) materials may be used in many optical-electronic systems and other next-generation defense technologies. With the importance of NLO materials, a series of push−pull architecture (D-π-A) derivatives (**DTMD2**−**DTMD6**) were devised from **DTMR1** through structural alteration of different efficient donor heterocyclic groups. Density functional theory-based computations were executed at the MPW1PW91/6-31G(d,p) level to explore the NLO behavior of the derivatives. To investigate the optoelectronic behavior of the said compounds, various analyses like the frontier molecular orbital (FMO), global reactivity parameters, density of state (DOS), absorption spectra (UV−vis), natural bond orbital, and transition density matrix (TDM) were performed. The derivatives have a smaller band gap (2.156−1.492 eV) and a larger bathochromic shift (λ_{max} = 692.838−969.605 nm) as compared to the reference chromophore (ΔE = 2.306 eV and λ_{max} = 677.949 nm). FMO analysis revealed substantial charge conduction out of the donor toward the acceptor via a spacer that was also shown by TDM and DOS analyses. All derivatives showed promising NLO results, with the maximum amplitude of linear polarizability $\langle\alpha\rangle$ and first (β_{total}) and second (γ_{total}) hyperpolarizabilities over their reference chromophore. **DTMD2** contained the highest β_{total} (7.220×10^{-27} esu) and γ_{total} (1.720×10^{-31} esu) values corresponding with the reduced band gap (1.492 eV), representing potential futures for a large NLO amplitude. This structural modification through the use of various donors has played a significant part in achieving promising NLO behavior in the modified compounds.

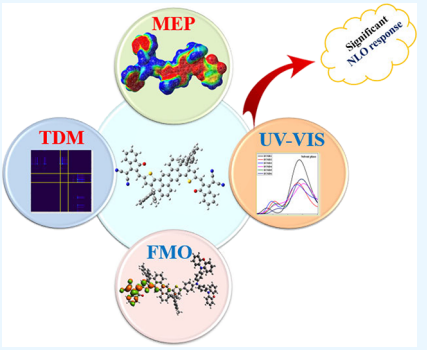

INTRODUCTION

Advancement in the progression of nonlinear optical (NLO) constituents is substantial in applied and fundamental research.[1] Experimental and theoretical communities have widely explored NLO substances because of their suitability in various areas such as nuclear science, chemical dynamics, medicine, surface interface studies, solid-state physics, material science, biophysics, and a wide range of optical devices.[2−5] Nowadays, it is quite challenging and substantial for scientists to plan novel efficacious NLO materials with improved properties by designing different organic and inorganic systems.[6,7] Notably, organic NLO compounds are considered advantageous over inorganic ones due to their fascinating properties such as larger molecular polarizability, enhanced electronic penetration, and rapid response times.[8] The organic compounds possess an electric charge delocalization due to a π-bond system, which endows them with enhanced nonlinear optical properties.[9−12] Organic compounds possessing donor−π-bridge−acceptor (D-π-A) configuration exhibit rapid response time and excellent NLO properties, making them an ideal candidate in various research regions, for example, optical memory/modulation, biophysics, molecular switching, laser, biophysics, and surface interface science.[8,13] The π-electron delocalization within the main configuration of the molecule creates the polarization in materials,[14−16] which drives the intermolecular charge transfer (ICT) and originates the transmission of electronic cloud through the donor−acceptor via π-linkers in the NLO materials, establishing a "push−pull" mechanism.[17−19] It is difficult to modify the fundamental D-A frameworks to create new high-performance NLO materials.[20−22] Organic compounds having substantial conjugated delocalized electron densities can be structurally modified to tune the second- and third-order nonlinear optics materials.[23,24] According to past studies, donor (D) and acceptor (A) moieties are important in achieving the necessary ground-state charge imbalance.[25−27]

Among the until-reported organic compounds, fullerene and its conjugated derivatives have gained widespread attention and are the most commonly used NLO molecules.[28−30] Fullerenes exhibit enhanced NLO properties due to the extensive charge delocalization.[30,31] Even though fullerene has

Received: October 1, 2023
Revised: November 7, 2023
Accepted: December 12, 2023
Published: January 8, 2024

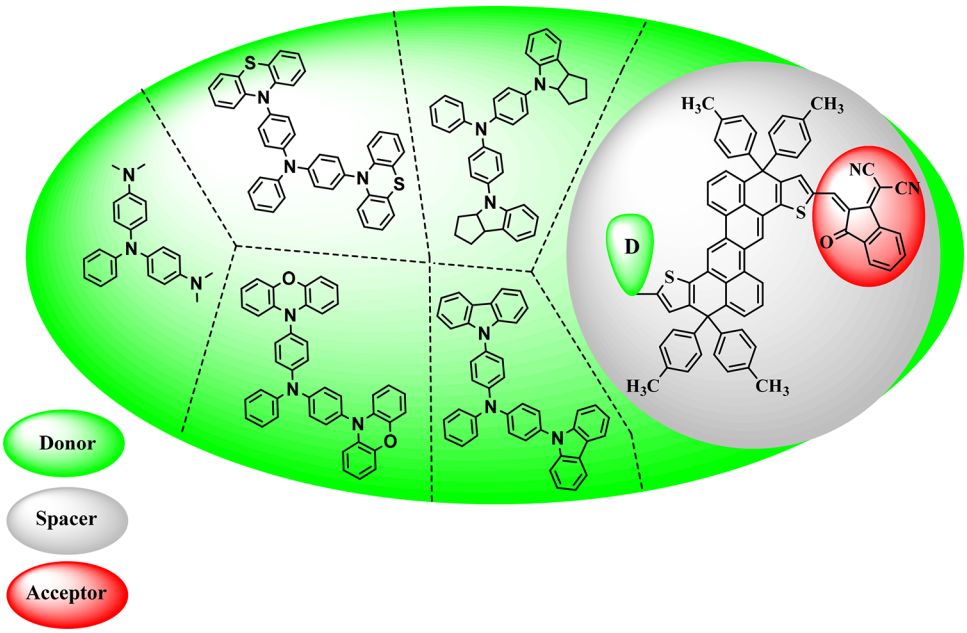

Figure 1. Schematic depiction of reference and its derivatives by alteration of the donor motif.

several important applications in optoelectronics, however, disadvantages such as low electrical conductivity and electron mobility may limit its use in perovskite solar cells.[32,33] In the last few decades, nonfullerene acceptors (NFAs) have been proposed as promising optoelectronic materials and have displayed abundant opportunities to meet the challenges in the development of NLO materials. More importantly, they have occupied the center of attention from fullerene derivatives due to various remarkable properties such as facile synthesis, exceptional stability, tunable band gaps, and strong light absorption capabilities.[34] The nonlinear characteristics of NFA compounds with D-π-A structural configuration can be efficiently modified by replacing appropriate D as well as A parts in addition to π-spacers at suitable locations.[35,36] There is abundant specified structural configuration in the literature, such as D-A, A-π-D-π-A, D-π-A, D-π-A-π-D, D-D-π-A, and D-A-π-A where "D" represents the donor region, "π" symbolizes the spacer, and "A" stands for the acceptor part. These configurations promote effective transmission among the D and units to construct an efficient push−pull framework. This creates a well-established NLO response by creating a reduction in the band gap, an increase in asymmetric electronic charge dissemination, and a bathochromic shift of the absorption spectra.[37] NFA molecules are thought to be very important in the field of nonlinear optics.[38] For this reason, masses of NFA species have been investigated in previous years to explore their photoelectrochemical characteristics. From the literature, it is examined that extended donors such as *N*,*N*-dialkylaniline,[39] indoline, phenothiazine, phenoxazine, and carbazole play an efficient role in tunning the NLO properties of NF chromophores. The resonating structures of aforementioned donors can easily tune HOMO/LUMO energy levels, allowing for precise control over the electronic properties to match those of acceptor materials. This characteristic enables efficient charge transfer and enhances the overall performance of organic electronic devices. Additionally, their high charge mobility facilitates fast and effective charge transport, vital for the operation of organic field-effect transistors and organic photovoltaic cells.[40] The synthetic versatility of extended donor derivatives enables the incorporation of various functional groups, enabling fine-tuning of their solubility, stability, and electronic properties to meet specific device requirements. Moreover, their excellent thermal stability ensures structural integrity and functionality during device fabrication and operation. The solution processability of these materials, owing to their solubility in common organic solvents, facilitates scalable and cost-effective manufacturing processes for large-area and flexible electronic devices. This compatibility with various device architectures, such as bulk heterojunction solar cells, organic light-emitting diodes, and organic photodetectors, underscores their potential for diverse organic electronic and optoelectronic applications. By leveraging these advantages, researchers can further harness the capabilities of extended donors to drive advancements in the field of organic electronics.[41]

Inspired by the previous studies and unique optoelectronic properties of π-conjugated NF-derived chromophores, we choose a chrysene-based, Z-shaped electron acceptor molecule as a reference (**DTMR1**) compound to design a series of chromophores (**DTMD2**−**DTMD6**) for NLO materials. The current work aims to build innovative NLO substances using a push−pull (D-π-A) structure from A-π-A. The new molecules (**DTMD2**−**DTMD6**) are created by swapping out the one-side end-capping acceptor unit with extended donor moieties, such as *N*,*N*-dialkylaniline (**DTMD2**), indoline (**DTMD3**), carbazole (**DTMD4**), phenothiazine (**DTMD5**), and phenoxazine (**DTMD6**) to investigate their NLO features theoretically. The current research explores the effects of the various donor moieties on the structural−property relationship and the NLO properties. Various quantum chemical techniques such as natural bonding orbitals (NBOs), frontier molecular orbitals (FMOs), density of states (DOSs), and global reactivity parameters (GRPs) have been considered using density functional theory (DFT) and time-dependent DFT (TD-DFT) computations, which prudent that the designed Z-shaped series of chromophores are better NLO materials than their reference. It is anticipated that the ongoing research will

https://doi.org/10.1021/acsomega.3c07596
ACS Omega 2024, 9, 3596−3608

play a significant role in assisting both theoretical and experimental scientists in the domain of nonlinear technology.

RESULTS AND DISCUSSION

In the current investigation, six novel Z-shaped chrysene-derived molecules (**DTMD2−DTMD6**) have been tailored by swapping the one-side acceptor unit with donor groups in **DTMR1**[42] to develop a push−pull architecture (see Figure 1), to obtain efficient NLO materials. The donor moiety utilized to tailor the compounds that are in **DTMD2** is named as *N*1-(4-(dimethylamino)phenyl)-*N*4,*N*4-dimethyl-*N*1-phenylbenzene-1,4-diamine (**NDP**); in **DTMD3**, *N*-phenyl-4-(1,3,3a,8b-tetrahydrocyclopenta[*b*]indol-4(2*H*)-yl)-*N*-(4-(1,3,3a,8b-tetrahydrocyclopenta[*b*]indol-4(2*H*)-yl)phenyl)aniline (**NTA**); in **DTMD4**, *N*-(4-(9*H*-carbazol-9-yl)phenyl)-4-(9*H*-carbazol-9-yl)-*N*-phenylaniline (**NCP**); in **DTMD5**, *N*-(4-(10*H*-phenothiazin-10-yl)phenyl)-4-(10*H*-phenothiazin-10-yl)-*N*-phenylaniline (**NPP**); and in **DTMD6**, *N*-(4-(10*H*-phenoxazin-10-yl)phenyl)-4-(10*H*-phenoxazin-10-yl)-*N*-phenylaniline (**NPA**), as shown in Figure S1. The optimized and chemDraw structures of **DTMR1** and **DTMD2−DTMD6** compounds are displayed in Figures S2 and S3. The DFT calculations for **DTMR1** and **DTMD2−DTMD6** compounds were executed via the MPW1PW91/6-31G(d,p) functional to assess the effect of different donors on the optical nonlinearity of said chromophores.

Frontier Molecular Orbitals (FMOs) and Global Reactivity Parameters (GRPs). The FMO analysis is substantially used to investigate the band gap energies, chemical stability, and electronic and optical behavior of organic systems.[43−46] The FMO energy difference (E_{gap} = E_{LUMO}−E_{HOMO}) of chromophores is associated with the extent of softness, hardness, reactivity, and dynamic stability of molecules.[47,48] Normally HOMOs entail the capability of giving electrons, whereas the LUMOs prompt to accept electrons from nucleophiles.[49] Molecules having less HOMO/LUMO energy gap are thought to be soft, are reactive with greater charge transference rate (CTR), and exhibit significant NLO properties and vice versa.[47,49,50] It has been examined from many reports that the band gap between the orbitals can be reduced by structural modification with effective electron-withdrawing and donating units in an organic system such as in nonfullerene chromophores. Herein, we calculated the molecular orbital (E_{LUMO}/E_{HOMO}) energies and their energy gap (E_{gap} = E_{LUMO}−E_{HOMO}) for **DTMR1** and **DTMD2−DTMD6** compounds at the MPW1PW91/6-31G(d,p) level to understand the result of various electron-donating units on molecular orbital energies and charge transference rate. The energies of HOMO/LUMO along with energy gaps are presented in Table 1.

It is evident from the calculations (Table 1) that reference compound **DTMR1** exhibits HOMO/LUMO energies of −5.698/−3.392 eV, respectively, with an energy difference of 2.306 eV, which are in good harmony with experimental results (E_{LUMO}/E_{HOMO} = −3.86/−5.49 eV). The HOMO/LUMO energies of **DTMD2−DTMD6** are examined as −4.652/−3.160, −5.052/−3.305, −5.245/−3.192, −5.348/−3.192, and −5.088/−3.191 eV, respectively. The modified compounds displayed reduced band gaps in the range of 1.492−2.156 eV in contrast to the reference **DTMR1** (2.306 eV). Triphenylamine derivatives exhibit sufficient hole transportation, extended conjugation, and a rigid plane, hence demonstrating promising characteristics from dye-sensitized solar cells (DSSCs) to electro-optics.[51−57] The HOMO energy values of designed compounds are quite high, while the LUMO values of designed molecules are low in contrast with reference **DTMR1**. Due to a rise in HOMO and a drop in LUMO, the resulting energy gap narrows in the proposed molecules (**DTMD2−DTMD6**), enabling a rapid transfer of charge between molecular orbitals.

Table 1. Calculated HOMO and LUMO Energies and Energy Gap Reference (DTMR1) and Designed (DTMD2−DTMD6) Compounds[a]

compounds	E_{HOMO}	E_{LUMO}	ΔE
DTMR1	−5.698	−3.392	2.306
DTMD2	−4.652	−3.160	1.492
DTMD3	−5.052	−3.305	1.747
DTMD4	−5.245	−3.192	2.053
DTMD5	−5.348	−3.192	2.156
DTMD6	−5.088	−3.191	1.897

[a]Units in eV. E = energy, ΔE = E_{LUMO}−E_{HOMO}; LUMO = lowest unoccupied molecular orbital; HOMO = highest occupied molecular orbital.

The lowermost band difference is recorded in **DTMD2** (1.492 eV), in all probability due to proficient charge transmission out of the substituted highly electron-donating part, *i.e.*, dimethylamino, linked to triphenylamine, as shown in Figure 2. Compounds that possess double-donor motifs exhibit greater polarizability and hyperpolarizability contrary to a single-donor motif.[58] Regarding **DTMD3**, the band gap is deemed to be lesser than **DTMR1** but higher than **DTMD2** (1.747 > 1.492 eV), apparently because of the end-caped donor moiety indoline. Indoline compounds possess distinguished hole-migrating and electron-donating capabilities, therefore generally adapted in various D-π-A structures.[59−61] The addition of the donor moiety (**NTA**) in **DTMD3** justified the lesser E_{gap} value. Moreover, the HOMO/LUMO energy difference discovered in the **DTMD4** molecule is lesser than **DTMR1** (2.053 < 2.306 eV) because of the addition of substituted carbazole in the effective donor (**NCP**). Due to the enlarged mobility of holes as well as adequate photoconductivity, carbazole dyes are among the highly studied compounds.[62−64] The **DTMD5** molecule showed a smaller energy gap than **DTMR1** but a larger gap than **DTMD2**, **DTMD3**, **DTMD4**, and **DTMD6**, *i.e.*, the highest E_{gap} among all designed compounds at 2.156 eV. Phenothiazine does not demonstrate extraordinary donating capability; limited donating characteristics are entirely exhibited by N not S.[65] The last derivative **DTMD6** shows a band gap of 1.897 eV, which is attributed to the effective donor unit enclosed by the molecule (NPA). This might be due to the strong ability to donate electrons and exceptional electronic properties of the phenoxazine group. The electron-rich heteroatoms (N and O) contribute to the high electron-donating tendency in phenoxazine.[66] The ascending order of the energy gap (HOMO/LUMO) for the examined compounds is **DTMD2** < **DTMD3** < **DTMD6** < **DTMD4** < **DTMD5** < **DTMR1**.

Furthermore, the GRPs are determined by the energy difference (HOMO/LUMO), describing the stability and reactivity of the compounds.[18] The GRPs such as the global electrophilicity index (ω), global softness (σ), global hardness (η), ionization potential (IP), electronegativity (X), the chemical potential (μ), and the electron affinity (EA) for

https://doi.org/10.1021/acsomega.3c07596
ACS Omega 2024, 9, 3596−3608

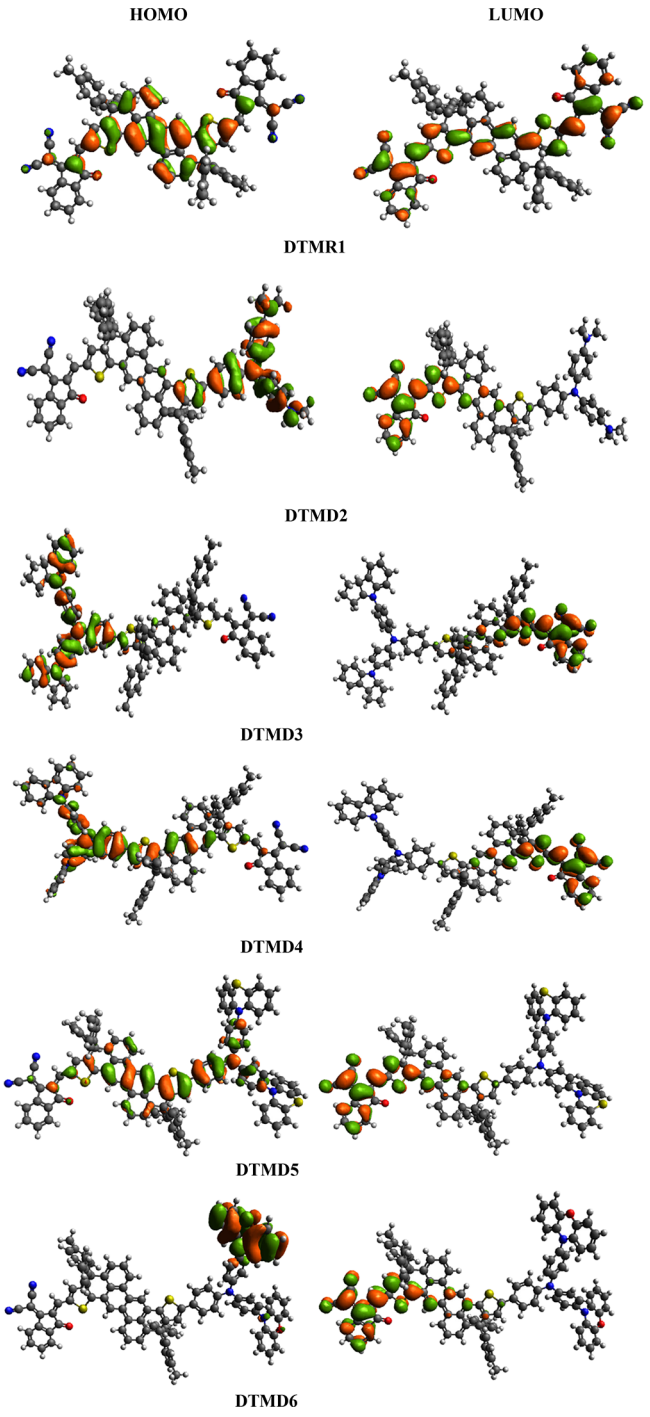

Figure 2. HOMOs and LUMOs of **DTMR1** and designed compounds (**DTMD2**−**DTMD6**).

entitled chromophores were predicted using FMOs,[67,68] and outcomes are tabulated in Table S1.

Table S1 reveals the direct correlation between a molecule's chemical hardness and its ΔE value and the inverse relationship between the molecule's overall softness and reactivity. A soft, unstable, and more reactive compound has a lower E value than a hard, stable, and less reactive system. The electronic cloud affinity to interact with an approaching atom is described chemically by a feature known as electronegativity.[69] Electron affinity and ionization potential values have been used to distinguish between a molecule's ability to accept and donate electrons.[70] The negative μ indicates molecular stability. These striking studies are beneficial to find the biological activity of the substances particularly in the area of experimental research.[71] The electron capturing capability is directly proportional to HOMO/LUMO energies and is described by electron affinity (E) values and its electron-donation capability, which can be stated by the IP values. The fact that the ionization potential value for **DTMR1** is higher than those for **DTMD2**−**DTMD6** further suggests that the derivatives tend to release electrons easily and need less energy to get polarized.[6] Between the designed chromophores, the highest softness is 0.670 Eh that is presented by **DTMD2**, which demonstrates maximum polarizability along with its improved reactivity. Meanwhile, a decrease in the softness value to 0.572 Eh is observed in the case of **DTMD3**. Further, the values are also decreased to 0.527, 0.487, and 0.463 Eh in **DTMD6**, **DTMD4**, and **DTMD5**, respectively. The least softness value (0.433 Eh) is seen in **DTMR1**, which represents its least reactivity with less polarizability. The ascending order of softness values for the studied compounds is **DTMD2** < **DTMD3** < **DTMD6** < **DTMD4** < **DTMD5** < **DTMR1**. The highest hardness (1.153 Eh) is detected in **DTMR1**, whereas the lowest hardness is observed in **DTMD2** at 0.736 Eh. Chemical potential follows the same trend relative to the hardness values. From the above-mentioned results, it can be deduced that the formulated compounds possess significant nonlinearity (see Tables S24−S28).

After the comparative analysis of various incorporated donor species, it has been observed that an efficient push−pull system is present in **DTMD2** and **DTMD3** with **NDP** and **NTA** donors, respectively, with the least band gap. Both electrons enrich donor compounds that generate strong intramolecular electronic exchange owing to reduced band gaps in D-π-A structures. Conversely, **DTMD4**, **DTMD5**, and **DTMD6** with **NCP**, **NPP**, and **NPA** donor groups, respectively, had greater band gaps of 2.053, 2.156, and 1.897 eV. This might be due to a less effective push−pull system as compared to the first two derivatives (**DTMD2** and **DTMD3**). This suggests that π-spacers connect electron-donating components to accepting units, facilitating the charge transmission among the D and A moieties. This makes the investigated compounds significant NLO constituents.[18]

Natural Bond Orbital (NBO) Analysis. NBO examination helps to explore the interaction, hydrogen bonding, inter- and intramolecular charge transfer, and delocalization of charge in organic moieties.[72,73] One of the most significant characteristics of the NBO analysis is that it gives an insight into the electronic charge delocalization and its transmission out of D to A in D-π-A configuration.[74] Due to the above-mentioned features, the NBO study was achieved to estimate the inter- and intramolecular modifications such as conjugative interactions, hydrogen bonding, and electronic delocalization in **DTMR1** and **DTMD2**−**DTMD6**. Tables S2−S7 present the results in tabular form. Stabilization energy values as well as conjugative interactions were obtained utilizing second-order perturbation theory.[75] Equation 1 was used to compute the stabilization energy $E^{(2)}$ related to charge delocalization from $i \rightarrow j$ for each donor (i) and acceptor (j).

$$E^{(2)} = \Delta E_{i,j} = q_i \frac{(F_{i,j})^2}{(\varepsilon_j - \varepsilon_i)} \quad (1)$$

https://doi.org/10.1021/acsomega.3c07596
ACS Omega 2024, 9, 3596−3608

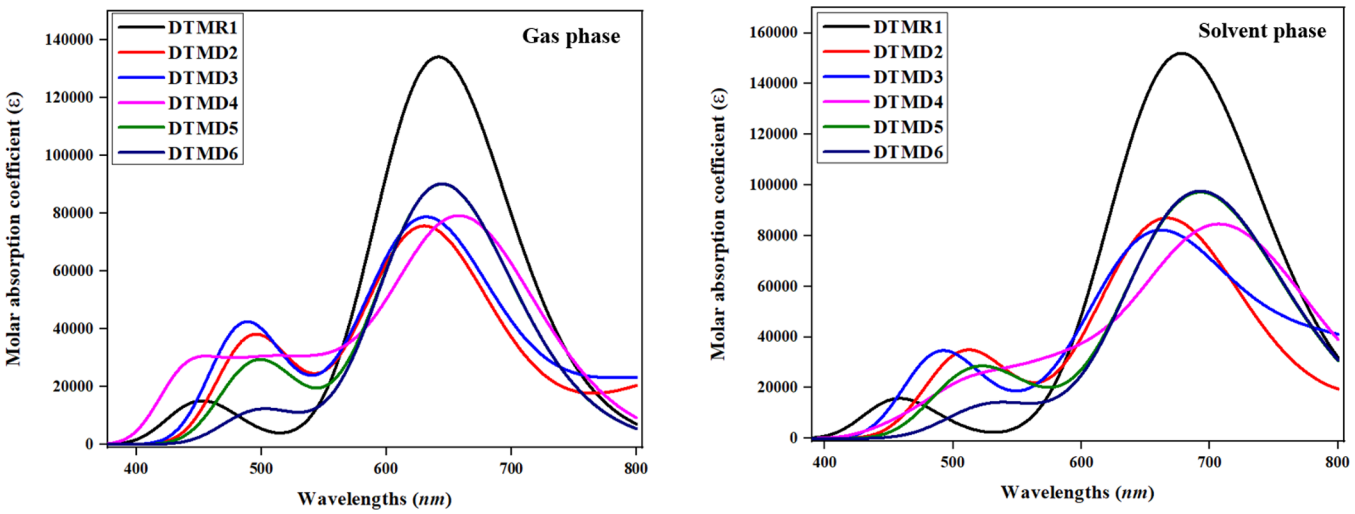

Figure 3. UV−vis plots for **DTMR1** and **DTMD2**−**DTMD6** in the solvent (chloroform) and gaseous phase.

In eq 1, $E^{(2)}$ characterizes the stabilization energy, q_i is the donor orbital occupancy, $F_{i,j}$ is the off-diagonal, and E_i and E_j are the diagonal NBO Fock matrix elements. $\Delta E_{i,j}$ is the energy difference between E_i and E_j diagonal NBO Fock matrix elements. $E^{(2)}$ values are directly associated with the electron interactions among the source and acceptor species. The greater the value of $E^{(2)}$, the more intense the interaction among electron-deficient and electron-rich molecules.[76]

Generally, four diverse electronic transitions are observed, *i.e.*, $\sigma \rightarrow \sigma^*$, $\pi \rightarrow \pi^*$, LP $\rightarrow \sigma^*$, and LP $\rightarrow \pi^*$, due to orbitals overlapping. Among the different electronic transitions, the $\pi \rightarrow \pi^*$ is the most reliable transition.

It is revealed from Table S8 that the maximum $\pi \rightarrow \pi^*$ transition in **DTMR1** arises at 28.73 kcal/mol for π (C28−C29) $\rightarrow \pi^*$ (C59−C60). However, the least $E^{(2)}$ for $\pi \rightarrow \pi^*$ arises as 0.79 kcal/mol for π (C137−N138) $\rightarrow \pi^*$ (C135−N136). Additionally, σ (C59−H101) $\rightarrow \sigma^*$(C29−S30) has the highest $\sigma \rightarrow \sigma^*$ transition with an $E^{(2)}$ of 9.09 kcal/mol. σ (C64−C113) $\rightarrow \sigma^*$(C60−C64) observes the minimum $E^{(2)}$ corresponding to the $\sigma \rightarrow \sigma^*$ transition. At 26.72 kcal/mol $E^{(2)}$ by LP2 (S27), the highest LP2 $\rightarrow \pi^*$ transition is detected (C20−C21). An $E^{(2)}$ of 13.36 kcal/molby LP1 (N112) $\rightarrow \sigma^*$ (C108−C111) is the maximum value of the same transition.

In **DTMD2**, the highest $\pi \rightarrow \pi^*$ transition is detected at 29.8 kcal/mol $E^{(2)}$ by π (C28−C29) $\rightarrow \pi^*$ (C59−C60). The minimum $\pi \rightarrow \pi^*$ transitions involve π (C8−C11) $\rightarrow \pi^*$ (C31−C37) with an $E^{(2)}$ of 0.55 kcal/mol. Furthermore, the maximum $E^{(2)}$ of 9.21 kcal/mol for the $\sigma \rightarrow \sigma^*$ transition involves σ (C59−H97) $\rightarrow \sigma^*$ (C29−S30). Meanwhile, the least $\sigma \rightarrow \sigma^*$ $E^{(2)}$ is 0.5 kcal/mol, displayed by σ (C121−H126) $\rightarrow \sigma^*$(C125−N128). The highest $E^{(2)}$ value for the LP $\rightarrow \pi^*$ transition is observed to be 43.43 kcal/mol by LP1 (N150) $\rightarrow \pi^*$ (C142−C146). The highest $E^{(2)}$ value for the above transition is 21.97 kcal/mol by LP2 (O62) $\rightarrow \sigma^*$(C61−C108).

The highest $\pi \rightarrow \pi^*$ transition for **DTMD3** is 29.63 kcal/mol involving π (C28−C29) $\rightarrow \pi^*$(C59−C60). Meanwhile, the least $E^{(2)}$ value for the $\pi \rightarrow \pi^*$ transition is 0.53 kcal/mol by π (C8−C11) $\rightarrow \pi^*$(C31−C37). In addition, σ (C59−H97) $\rightarrow \sigma^*$(C29−S30) discloses the maximum $E^{(2)}$ value for the $\sigma \rightarrow \sigma^*$ transition at 9.18 kcal/mol. The minimum $E^{(2)}$ value is presented by σ (C29−C59) $\rightarrow \sigma^*$ (C29−S30). The maximum $E^{(2)}$ value for the LP1 $\rightarrow \pi^*$ transition is 44.03 kcal/mol by LP1 (N150) $\rightarrow \pi^*$ (C161−C162). The maximum $E^{(2)}$ value is 21.97 kcal/mol exhibited by LP2 (O62) $\rightarrow \sigma^*$ (C61−C108).

For **DTMD4**, the highest $E^{(2)}$ for the $\pi \rightarrow \pi^*$ transition is reported to be 29.43 kcal/mol due to π (C28−C29) $\rightarrow \pi^*$(C59−C60). Although, the least $E^{(2)}$ for $\pi \rightarrow \pi^*$ is 0.57 kcal/mol by the π (C13−C14) $\rightarrow \pi^*$ (C32−C38) transition. Moreover, σ (C59−H97) $\rightarrow \sigma^*$ (C29−S30) discloses the maximum $E^{(2)}$ value for the $\sigma \rightarrow \sigma^*$ transition at 9.16 kcal/mol. The minimum $\sigma \rightarrow \sigma^*$ transition is reported in σ (C61−C108) $\rightarrow \sigma^*$ (C60−C61) at 0.5 kcal/mol. The highest LP1 $\rightarrow \pi^*$ transition is 42.5 kcal/mol $E^{(2)}$ by LP1 (N150) $\rightarrow \pi^*$ (C171−C173). The maximum $E^{(2)}$ value of the equivalent transition is reported at 21.96 kcal/mol by LP2 (O62) $\rightarrow \sigma^*$ (C61−C108).

For **DTMD5**, the highest $\pi \rightarrow \pi^*$ $E^{(2)}$ is reported at 29.5 kcal/mol by π (C28−C29) $\rightarrow \pi^*$(C59−C60). Nonetheless, the least $E^{(2)}$ for the $\pi \rightarrow \pi^*$ transition is found at 0.6 kcal/mol by π (C32−C38) $\rightarrow \pi^*$(C13−C14). Furthermore, σ (C59−H97) $\rightarrow \sigma^*$(C29−S30) displays the maximum $\sigma \rightarrow \sigma^*$ transition value for $E^{(2)}$ at 9.19 kcal/mol. The minimum $\sigma \rightarrow \sigma^*$ transition is noticed in σ (C61−C108) $\rightarrow \sigma^*$(C60−C61) at 0.5 kcal/mol. The maximum LP $\rightarrow \pi^*$ transition is detected at 30.58 kcal/mol $E^{(2)}$ by LP1 (N149) $\rightarrow \pi^*$ (C151−C152). The maximum value of $E^{(2)}$ is observed at 21.97 kcal/mol by LP2 (O62) $\rightarrow \sigma^*$ (C61−C108).

For **DTMD6**, the maximum $\pi \rightarrow \pi^*$ transition is at 29.43 kcal/mol $E^{(2)}$ by π (C28−C29) $\rightarrow \pi^*$(C59−C60). The minimum $E^{(2)}$ for $\pi \rightarrow \pi^*$ transitions is exhibited by π (C8−C11) $\rightarrow \pi^*$ (C31−C37) at 0.63 kcal/mol. Furthermore, the maximum $E^{(2)}$ value of 9.17 kcal/mol for $\sigma \rightarrow \sigma^*$ transitions is exhibited by σ (C59−H97) $\rightarrow \sigma^*$ (C29−S30). Meanwhile, the least $\sigma \rightarrow \sigma^*$ transition $E^{(2)}$ value is 0.5 kcal/mol by σ (C29−S30) $\rightarrow \sigma^*$ (C13−C14). The maximum LP1 $\rightarrow \pi^*$ transition is detected at 39.05 kcal/mol $E^{(2)}$ by LP1 (N150) $\rightarrow \pi^*$ (C171−C173). The maximum $E^{(2)}$ value is detected at 21.97 kcal/mol by LP2 (O62) $\rightarrow \sigma^*$ (C61−C108). In the LP2 (O62) $\rightarrow \sigma^*$ (C61−C108) transition, the same $E^{(2)}$ is observed, *i.e.*, 21.97 kcal/mol in all the designed compounds (**DTMD2**−**DTMD6**). The detailed transitions for all compounds are illustrated in Tables S2−S7. The preceding discussion proves that the NBO findings of all the computed chromophores are parallel to one another. Therefore, hyper-

https://doi.org/10.1021/acsomega.3c07596
ACS Omega 2024, 9, 3596−3608

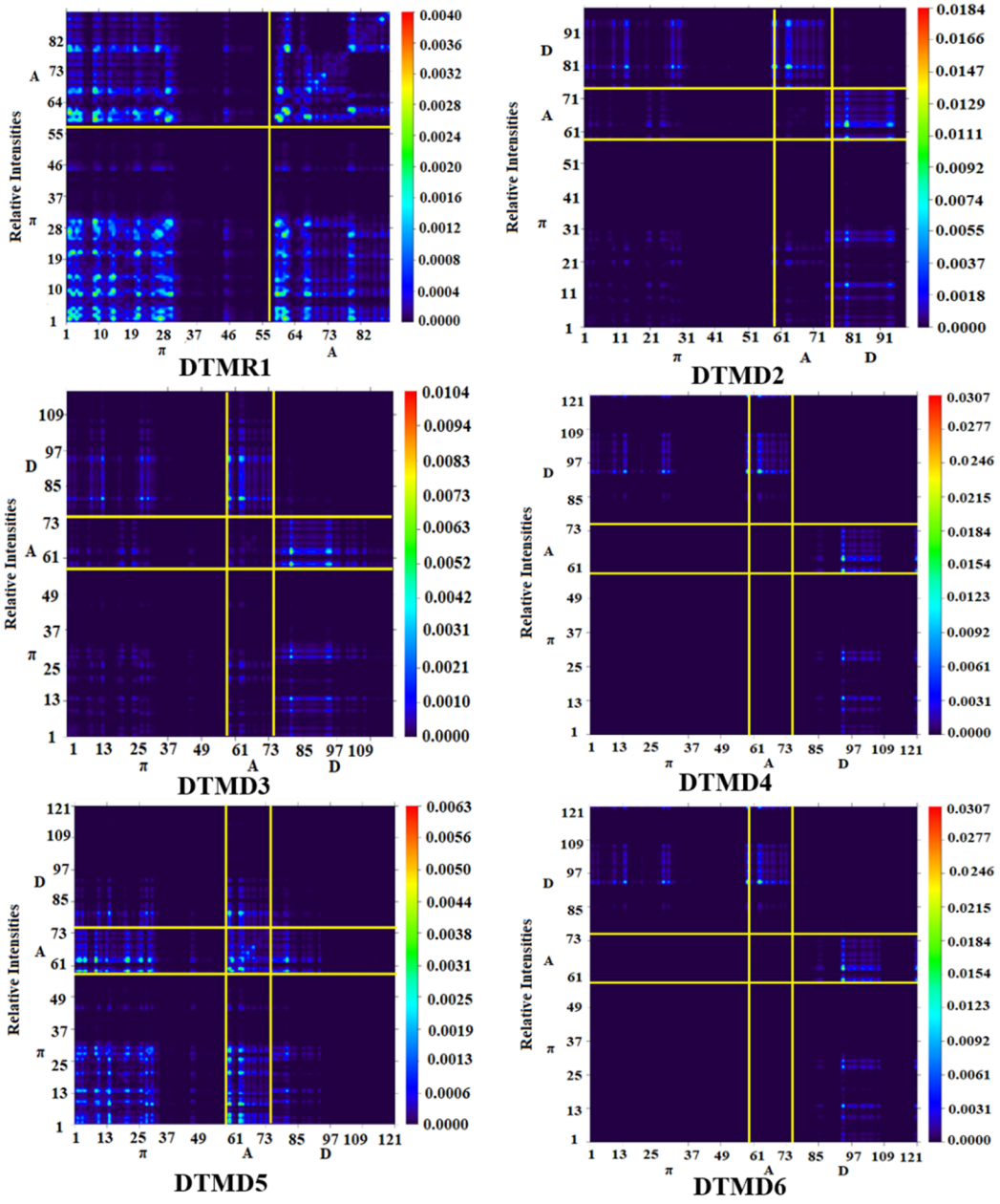

Figure 4. TDM graphs of the reference (**DTMR1**) and the designed compounds (**DTMD2**−**DTMD6**).

conjugation and ICT greatly impact the molecular stability of the formulated compounds.

Absorption Analysis. The optical characteristics of the designed and reference compounds were evaluated by performing absorption analysis in the solvent (chloroform) and gaseous phase. The computed values for absorption maxima λ_{max}, oscillator strength, contributing molecular orbitals, and excitation energy are tabulated in Table S21. Meanwhile, further information is given in Tables S9−S20. It is observed from the results that the conjugation accompanied by the electron-withdrawing terminal unit is responsible for a high bathochromic shift in UV absorption spectra,[77] as shown in Figure 3. Our designed chromophores with D-π-A configuration possess numerous optoelectronic advantages due to the prolonged π-conjugation.

It is observed from the values shown in Table S21 that the **DTMD2** compound possesses a small λ_{max} in the gaseous phase (883.702 nm) while being higher in chloroform (969.605 nm) with excitation energy values of 1.403 and 1.279 eV and oscillator strengths of 0.384 and 0.413, respectively. This is due to the interaction of acceptor units with the solvent phase. This interaction has lowered the energy difference between the ground state and excited state as well as brought about the bathochromic shift resulting in better optical properties. This is most likely due to the addition of dimethylamino in the donor part that correspondingly induced high electron density transference out of HOMO toward LUMO molecular orbitals because of the least energy gap and red shift. The intended values of λ_{max} are found in the range of 602.504−883.702 nm in the gas phase and 677.949−969.605 nm in the chloroform solvent for all the compounds. The highest λ_{max} of the solvent and gas phase are comparable and close to each other because of the incidence of more extended π-conjugation. The compounds **DTMD2**, **DTMD3**, and

https://doi.org/10.1021/acsomega.3c07596
ACS Omega 2024, 9, 3596−3608

DTMD6 showed a bathochromic shift in absorption maxima, which could be attributed to the introduction of extra functional groups in end-capped moieties of these compounds. The molecule **DTMD3** reflected the second bathochromic shift in the absorption spectrum (λ_{max} = 831.656 nm) in the gaseous phase while having λ_{max} = 820.919 nm in chloroform with activation energies of 1.491 and 1.510 eV and f of 0.303 and 0.459, respectively. This is because of the presence of indoline as a donor group and reduced band gap, which however is greater than **DTMD2**. **DTMD6** manifests λ_{max} in the gaseous phase and chloroform at 712.835 and 719.119 nm, with excitation energies of 1.739 and 1.724 eV and f of 0.000 and 0.002, respectively. The presence of heteroatoms (N and O) on the phenoxazine group in the donor moiety reduces the band gap and increases wavelength, hence high donating tendency. The **DTMD4** (λ_{max} = 661.174 nm in the gaseous phase while λ_{max} = 711.403 nm in chloroform) and **DTMD5** (λ_{max} = 602.504 nm in the gaseous phase while λ_{max} = 692.838 nm in chloroform) molecules exhibit a small gloomy shift, but they still display a bathochromic shift in the absorption spectrum in comparison to **DTMR1** maximum absorption. Excitation energies in the gaseous phase and chloroform displayed by **DTMD4** and **DTMD5** are 1.875 as well as 1.743 eV and 2.058 as well as 1.790 eV and oscillator strengths of 1.064 as well as 1.135 and 0.00 as well as 1.340, respectively. The donor moiety containing the carbazole group in **DTMD4** and the phenothiazine group in **DTMD5** shows a high energy gap which is lesser than **DTMR1**. This is due to their less electron-donating tendency. The descending order of λ_{max} values in the gas phase and chloroform is **DTMD5** > **DTMR1** > **DTMD4** > **DTMD6** > **DTMD3** > **DTMD2** in nanometers. The absorption spectra of the **DTMD2**−**DTMD6** compounds lay in the UV region in both the gaseous phase and chloroform solvent, which demonstrates their good NLO properties (Figure 3).

Transition Density Matrix (TDM). TDM examination was done to reveal the electronic excitations, electron−hole pair delocalization, and transitions within the molecule, and the results were computed by using MPW1PW91/6-31G(d,p). Because of the little influence by H atoms in the transition, their impact was overlooked and neglected.[78] The reference chromophore was fragmented into two parts, *i.e.*, acceptor and π-spacer, while the designed chromophores are distributed into three segments, *i.e.*, acceptor, π-bridge, and donor for TDM analysis. The emission spectra of **DTMR1** and **DTMD2**−**DTMD6** displayed in Figure 4 are used to identify the electron coherence and the relationship between different fragments of the molecule. The TDM pictographs (see Figure 4) represent the number of atoms along the x axis and on the left side of the y axis, while its right side depicts the electron density flow.

FMO analysis demonstrated the considerable charge transfer in reference and designed molecules and was observed in the heat map of the TDM. The charge transfer rate was affected by the structure of the molecule and the variation in end groups. There was substance electronic charge distribution in the core of **DTMR1**, **DTMD4**, and **DTMD5**, while the central unit of **DTMD2**, **DTMD3**, and **DTMD6** had little or no electronic cloud. Among all the designed molecules, **DTMD4** and **DTMD5** demonstrated significant charge distribution properties.

Another means to explain the working efficiency and optoelectronic properties of NLO compounds is binding energy. Binging energy is inversely related to exciton dissociation and is directly proportional to the Coulombic force of attraction among electron−hole pairs in the molecule.[78,79] The value of E_b was calculated by using eq 2, and its results are depicted in Table 2.

$$E_b = E_{H-L} - E_{opt} \quad (2)$$

Table 2. Band Gap (E_{H-L}), First Singlet Excitation Energy (E_{opt}), and Exciton Binding Energies (E_b)[a]

compounds	E_{H-L} (eV)	E_{opt} (eV)	E_b (eV)
DTMR1	2.306	1.829	0.477
DTMD2	1.492	1.279	0.213
DTMD3	1.747	1.510	0.237
DTMD4	2.053	1.743	0.31
DTMD5	2.156	1.790	0.366
DTMD6	1.897	1.724	0.173

[a]Units in eV.

The calculated E_b results of all the modulated molecules **DTMD2** (E_b = 0.213 eV), **DTMD3** (E_b = 0.237 eV), **DTMD4** (0.310 eV), **DTMD5** (E_b = 0.366 eV), and **DTMD6** (E_b = 0.173 eV) are lower than **DTMR1** (E_b = 0.477eV). **DTMD6** has the lowest value of binding energy, which illustrates the excessive charge transfer and maximum charge separation efficiency of this compound. The decreasing order of E_b is **DTMR1** > **DTMD5** > **DTMD4** > **DTMD3** > **DTMD2** > **DTMD6**. From the results, it is predicted that all the designed compounds reveal outstanding photovoltaic properties such as high current charge density and high charge separation. Moreover, the outcomes of E_b and TDM are in good correlation with each other.

Density of States (DOS). The DOS denotes various types of states that electrons can inhabit at a quantized energy level, *i.e.*, electronic states per unit volume per unit energy (DOSs) to support the FMO analysis.[37] The overall energy levels scattering as a function of energy and the energy gap can be calculated using density of state (DOS) calculations.[80] The DOS maps of **DTMR1** and **DTMD2**−**DTMD6** are plotted at the MPW1PW91/6-31G(d,p) and presented in Figure S4 and Table S22. Each compound is made up of three major components: a donor, a spacer, and an acceptor.

In the case of the reference compound (**DTMR1**), acceptor contributions for HOMO and LUMO are 60.6 and 19.3% respectively. Meanwhile, the donor contributions are 0.6, 65.1, 0.5, 0.5, and 0.5% to the HOMO while 88.6, 92.3, 63.0, 36.9, and 100.0% to the LUMO for **DTMD2**−**DTMD6**, respectively (Table S22). These contributions reveal that changing different efficient donor moieties in different compounds (**DTMD2**−**DTMD6**) plays a key part in electronic cloud transfer in various ways. In the same manner, acceptor contributions for HOMO are 60.6, 64.9, 0.5, 64.9, 64.6, and 65.1% and for LUMO are 19.3, 0.6, 0.4, 2.3, 4.6, and 0.0% for all designed compounds. Likewise, the π-spacer contributes to HOMO of 39.4, 34.5, 34.4, 34.6, 34.9, and 34.5% and LUMO of 80.7, 10.9, 7.4, 34.6, 58.5, and 0.0% for **DTMR1** and **DTMD2**−**DTMD6** compounds, respectively (Table S22). For compound **DTMD2**, the maximum charge density placed on HOMO in the π-spacer is −12.5 eV whereas the maximum charge density found in LUMO over the acceptor is 5 eV. The **DTMD3** compound showed the highest charge density of the donor in HOMO at −9.3 eV, while in LUMO, it is found on the π-spacer at 4 eV. In **DTMD4**, the highest charge density is

https://doi.org/10.1021/acsomega.3c07596
ACS Omega 2024, 9, 3596−3608

found in the donor at −12.5 eV, while in LUMO, it is found on the π-spacer at 4 eV. In the **DTMD5** compound, the maximum charge location in HOMO on the donor is at −13.5 eV, while in LUMO, it is found at 4.5 eV. In the **DTMD6** compound, the maximum charge density of the donor was found at −13.5 eV in HOMO and in LUMO found in the π-spacer in LUMO at 3 eV. These energy values show the excellent charge transmission out of the donor toward the acceptor through the π-spacer.

Molecular Electrostatic Potential (MEP) Analysis. Exploring the MEP is essential for revealing the total charge density of a molecule at various charge sites. Moreover, the MEP plots explain the compound reactivity by predicting the electrophilic and nucleophilic locations of a molecule.[81,82]

To investigate the rationale behind the effective design of various new compounds, we executed MEP calculations on all the designed compounds at the MPW1PW91/6-31G(d,p). The theoretical investigation of MEP plots and their map of **DTMR1** and **DTMD2**−**DTMD6** (orange color, partially negative charge; red color, characterize electron-rich sites; yellow color, lightly electron-rich regions; green color, neutral sites; and blue color, positive charge) is depicted in Figure S5. It is noted that sulfur and oxygen signify electron-rich sites, while the blue sites indicate hydrogen atoms. Furthermore, the presence of red color on oxygen atoms supports the oxygen atoms' electronegative nature. The carbon and hydrogen atoms represent an electropositive nature owing to the presence of blue color and provide signals for nucleophilic attachment at these locations. The yellow color of sulfur atoms indicates that it has a less negative nature than oxygen. These findings demonstrate the efficiency of donor alteration for creating fullerene-free acceptor molecules for DFT.

Nonlinear Optical (NLO) Properties. NLO properties explain the concepts of linear response (polarizability $\langle\alpha\rangle$ and no linear response (first (β_{total}) and second hyperpolarizabilities (γ_{total}) based on fast electronic response)).[83] The optical response intensity has a direct relationship with the material's electronic properties. It is confirmed from the previous studies that a large value of linear polarizability contributes to the higher β_{total} values. Herein, Table 3 displays

Table 3. Dipole Moment, Average Polarizability, First Hyperpolarizability, and Second-Order Hyperpolarizability[a]

compound	μ_{total}	$\langle\alpha\rangle \times 10^{-22}$	$\beta_{total} \times 10^{-27}$	$\langle\gamma\rangle \times 10^{-32}$
DTMR1	0.791	2.640	0.061	2.463
DTMD2	1.755	2.903	7.220	1.720
DTMD3	1.396	3.195	5.156	1.122
DTMD4	3.354	3.133	2.899	3.819
DTMD5	3.580	3.157	2.665	3.180
DTMD6	3.157	3.105	2.637	3.047

[a] μ_{total} units in D; $\langle\alpha\rangle$, β_{total}, and γ_{total} units in esu.

the computed values of NLO parameters, such as average polarizability $\langle\alpha\rangle$, first (β_{total}) and second hyperpolarizability (γ_{total}), and dipole moment (μ_{total}) values of the reference and designed compounds. Tables S23−S28 discuss the other subsidizing tensors in detail.

The designed compounds (**DTMD2**−**DTMD6**) have a D-π-A configuration, which is created by modifying the donor part that exhibits an outstanding push−pull framework. The alternation of different donor moieties causes alteration in polarizability and band gap values.[69] The designed compound **DTMD5** possesses the highest value of μ_{total} (3.580 D), while **DTMR1** possesses the lowest value of μ_{total} (0.791 D), which corresponds to the highest global hardness value of **DTMR1** among all the derivatives. The highest value of μ_{total} in the case of **DTMD5** and its lower energy gap might be because of phenothiazine attached to the donor moiety, which has a powerful electron-withdrawing property. In **DTMR1**, **DTMD2**, and **DTMD4**, the major contributing tensor toward μ_{total} is along the y axis (μ_{yy}). However, for **DTMD2, DTMD3, DTMD5**, and **DTMD6**, the major contributing tensor is μ_{zz} toward μ_{total}. The decreasing order of the overall discovered dipole moments is as follows: **DTMD5** > **DTMD4** > **DTMD6** > **DTMD2** > **DTMD3**. Similarly, the decreasing order of the reference and designed compound's average linear polarizability is as follows: **DTMD3** > **DTMD5** > **DTMD4** > **DTMD6** > **DTMD2** > **DTMR1**.

The compound's polarity and its electronic properties are efficiently explained by the linear polarizability. The values of major contributing factors of $\langle\alpha\rangle$ are listed in Table S24, whereas $\langle\alpha\rangle$ values are enlisted in Table 3 (with units in esu). The dominant tensor contributing in average polarizability is along the x axis (α_x), which depicts that $\langle\alpha\rangle$ lies in this axis. Table 3 shows that **DTMD3** has dominant average polarizability, *i.e.*, 3.195×10^{-22} esu with $\alpha_{xx} = 4.921 \times 10^{-22}$ esu, $\alpha_{yy} = 2.816 \times 10^{-22}$ esu, and $\alpha_{zz} = 1.849 \times 10^{-22}$ esu in x, y, and z axes, respectively. Thus, the major contributing tensor is α_{xx} toward the average polarizability of all the compounds. A literature survey reveals the HOMO/LUMO gap effect molecular polarizability, with a smaller band gap proportional to considerable linear polarizability.

The designed compound **DTMD2** possesses the highest hyperpolarizability value (7.220×10^{-27} esu), which correlates to the highest electrophilicity index, chemical potential, and lowest ionization potential and electronegativity values in GRPs. Meanwhile, **DTMD6** possesses the lowest β_{total} value, which showed good charge transfer in **DTMD2** and poor charge transfer in **DTMD6** as illustrated by softness values (see Table S1). The introduction of the trimethylamine atom that bonded with substituted dimethylamino groups (as the electron donor) in **DTMD2** altered the electron-donating ability of the molecule, which resulted in efficiently high NLO values. In the case of **DTMD6**, the β_{total} value was found to be quite lower at 2.637×10^{-27} esu, as compared to **DTMD2** (7.220×10^{-27} esu). This is based on the fact that the existence of heteroatoms (N and O) in phenoxazine that bonded with the triphenylamine ring offers a remarkably lower amplitude of intramolecular interaction energy, and as a result, it enhances the NLO response. For compounds **DTMR1** and **DTMD4**−**DTMD6**, the major contributing tensors are β_{xxz} at 5.050×10^{-29}, 2.136×10^{-28}, 1.084×10^{-28}, and 6.862×10^{-29} esu, respectively. However, the derivatives **DTMD2** and **DTMD3** have dominant tensors as β_{xxy} with values of 5.666×10^{-28} and 1.841×10^{-28} esu, respectively. The electron delocalization and the HOMO/LUMO energy gap have an inverse relationship. If the electron delocalization is greater, then the HOMO/LUMO energy gap is smaller, and the hyperpolarizability (β_{total}) values in the designed compounds increase. Hence, β_{total} values correspond to the band gap, with the highest β_{total} of 7.220×10^{-27} esu, which is shown by the compound with the least band gap, *i.e.*, 1.492 eV. The first hyperpolarizability values of **DTMR1** and **DTMD2**−**DTMD6** are 6.075×10^{-29}, 7.220×10^{-27}, 5.156×10^{-27}, 2.899×10^{-27}, 2.665×10^{-27}, and 2.637×10^{-27}, respectively. The following

https://doi.org/10.1021/acsomega.3c07596
ACS Omega 2024, 9, 3596−3608

is the decreasing order of total values for all designed compounds: **DTMD2** > **DTMR1** > **DTMD3** > **DTMD4** > **DTMD5** > **DTMD6**. For the second hyperpolarizability $\langle\gamma\rangle$ values, the major contributing tensor for all the compounds is along the *x* axis, *i.e.*, γ_x. The highest value of $\langle\gamma\rangle$ is shown by **DTMD2** at 1.720×10^{-31} esu with a dominant tensor, *i.e.*, $\gamma_x = 1.695 \times 10^{-31}$ esu, whereas the least contribution toward $\langle\gamma\rangle$ is shown by γ_z at 2.604×10^{-34} esu.

The designed compounds' structural variations result in high polarizability and improved NLO parameters. The first hyperpolarizability values are discovered by reversing the order of E_{gap} values between the HOMO/LUMO orbitals. All of the designed compounds had significantly improved NLO properties, such as smaller band gaps, which explains why the designed compounds with a D-π-A architecture have more polarity than those with an A-π-A configuration.

A comparative analysis of our compounds is performed with urea ($\beta_{to} = 3.72 \times 10^{-30}$ esu)[84] and para-nitro aniline (*p*-NA), a protype molecule ($\beta_{tot} = 0.3610 \times 10^{-30}$ esu)[85] that is used as reference in the NLO study. All our compounds showed a significantly higher response than the urea molecule. Similarly, the hyperpolarizability values for **DTMR1** and **DTMD2**−**DTMD6** compounds, *i.e.*, 0.061×10^{-27}, 7.220×10^{-27}, 5.156×10^{-27}, 2.899×10^{-27}, 2.665×10^{-27}, and 2.637×10^{-27} esu, are higher than that of the *p*-NA molecule, respectively, which demonstrates that all designed compounds would be used as efficient NLO materials. Additionally, we also developed a comparative study with our previously reported similar analogue **DOCD2**.[86] Interestingly, all our compounds **DTMR1** and **DTMD2**−**DTMD6** exhibited 0.493×10^{-27}, 7.184×10^{-27}, 5.691×10^{-27}, 4.345×10^{-27}, 0.003×10^{-27}, and 3.736×10^{-27} esu times higher hyperpolarizability values, respectively. This comparative study illustrated that our compounds could be utilized as efficient NLO materials.

CONCLUSIONS

Herein, chrysene-based nonfullerene chromophores (**DTMD2**−**DTMD6**) have been formulated having a D-π-A structure from **DTMR1**. Fantastically, all computed compounds possessed less HOMO/LUMO energy gap as compared to **DTMR1**, with ascending order as **DTMD2** < **DTMD3** < **DTMD6** < **DTMD4** < **DTMD5** < **DTMR1**. Their UV-visible spectra described stronger absorption wavelengths (677.949−969.605 nm), consistent with less transition energy values in derivatives than that of the reference chromophore. The binding energy (E_b) indicated a significant impact by the donor part in lower transition energy values. TDM and DOS maps exploit significant transference of charge from the donor toward the acceptor through the linker. The **DTMD2**−**DTMD6** showed reduced E_b values (0.173−0.366 eV) compared to the reference **DTMR1** (0.477 eV), which infers less Coulombic forces with enhanced charge mobility in it. The values of $\langle\alpha\rangle$, β_{total}, and γ_{total} are observed significantly for the designed compounds in comparison to **DTMR1**. Favorable nonlinear behavior was observed in **DTMD2** [$\langle\alpha\rangle = 2.903 \times 10^{-22}$, $\beta_{total} = 7.220 \times 10^{-27}$, and $\gamma_{total} = 1.720 \times 10^{-31}$ esu)]. In conclusion, the efficient modeling of the chromophores with heterocyclic donor units resulted in promising nonlinearity qualifying for advanced optical technology.

COMPUTATIONAL METHODOLOGY

All the DFT calculations for chrysene-based Z-shaped compounds were performed via the Gaussian 09,[87] program. From the literature, we found out that Khan et al.[88] reported the photovoltaic properties of the **FCIC** chromophore via the DFT approach. In that report, they selected the MW1PW91/6-311G(d,p) functional[89,90] through the benchmark study between experimental and DFT values of λ_{max} at various functionals of the **FCIC** compound. Therefore, to investigate the nonlinear optical properties of **FCIC**, which is named **DTMR1**, utilized as a reference in the current study and its derivatives, we used the MW1PW91/6-311G(d,p) level. First of all, the geometrical optimization of all the studied compounds was done at the aforementioned functional and the lack of imaginary frequencies was assured for local minima, which confirmed the optimization of the structure. To uncover the electronic and optical characteristics of **DTMR1** and **DTMD2**−**DTMD6**, various analyses such as DOSs, NBOs, HOMO/LUMO band gaps, NPA, GRPs, UV−vis, TDM, and NLO were computed at the aforementioned functional. To interpret the data from outputs, different kinds of software like the Gauss View 5.0 program,[91] Avogadro,[92] Chemcraft,[93] Multiwfn,[94] and Origin[95] were used. Further, eqs 3−6 were employed to determine the dipole moment (μ_{total}),[81] linear polarizability $\langle\alpha\rangle$,[82,96] hyperpolarizability (β_{total}),[97] and second hyperpolarizability (γ_{total})[8] behavior of **DTMR1** and **DTMD2**−**DTMD6**.

$$\mu = (\mu^2_x + \mu^2_y + \mu^2_z)^{1/2} \tag{3}$$

$$\langle\alpha\rangle = 1/3\langle\alpha_{xx} + \alpha_{yy} + \alpha_{zz}\rangle \tag{4}$$

$$\beta_{total} = [(\beta_x^2 + \beta_y^2 + \beta_z^2]^{1/2} \tag{5}$$

Ten hyperpolarizability (β_{total}) tensors were aligned across the *x*, *y*, and *z* axes: β_{xxx}, β_{xyy}, β_{xzz}, β_{yyy}, β_{xxy}, β_{yzz}, β_{zzz}, β_{xxz}, β_{yyz}, and β_{xyz} by analyzing Gaussian output files.[83]

$$\gamma_{total} = \sqrt{\gamma_x^2 + \gamma_y^2 + \gamma_z^2} \tag{6}$$

where $\gamma_i = \frac{1}{15}\sum_j \left(\gamma_{ijji} + \gamma_{ijij} + \gamma_{iijj}\right) i, j = \{x, y, z\}$.

ASSOCIATED CONTENT

Supporting Information

The Supporting Information is available free of charge at https://pubs.acs.org/doi/10.1021/acsomega.3c07596.

UV−vis data (wavelengths, excitation energies, and oscillator strengths), MEP, NBO analysis, dipole moments, linear polarizabilities with major contributing tensors, the first hyperpolarizabilities (β_{tot}) and second hyperpolarizabilities (γ_{tot}) with their contributing tensors, ChemDraw structures and their IUPAC names, and optimized geometries of the reported compounds calculated using MPW1PW91/6-31G(d,p) (PDF)

AUTHOR INFORMATION

Corresponding Authors

Faiz Rasool − *Institute of Chemical Sciences, Bahauddin Zakariya University, Multan 60800, Pakistan;* orcid.org/0000-0002-7825-9667; Email: faizrasoolbzu@gmail.com

https://doi.org/10.1021/acsomega.3c07596
ACS Omega 2024, 9, 3596−3608

Ke Chen − *Department of Infectious Diseases, The Affiliated Hospital of Southwest Medical University, Luzhou 646000, China*; Email: chitty8705@sina.com

Authors

Gang Wu − *Department of Infectious Diseases, The Affiliated Hospital of Southwest Medical University, Luzhou 646000, China*

Iqra Shafiq − *Institute of Chemistry, Khwaja Fareed University of Engineering & Information Technology, Rahim Yar Khan 64200, Pakistan; Centre for Theoretical and Computational Research, Khwaja Fareed University of Engineering & Information Technology, Rahim Yar Khan 64200, Pakistan*

Shehla Kousar − *Institute of Chemistry, Khwaja Fareed University of Engineering & Information Technology, Rahim Yar Khan 64200, Pakistan; Centre for Theoretical and Computational Research, Khwaja Fareed University of Engineering & Information Technology, Rahim Yar Khan 64200, Pakistan*

Saba Abid − *Institute of Chemistry, Khwaja Fareed University of Engineering & Information Technology, Rahim Yar Khan 64200, Pakistan; Centre for Theoretical and Computational Research, Khwaja Fareed University of Engineering & Information Technology, Rahim Yar Khan 64200, Pakistan*

Norah Alhokbany − *Department of Chemistry, College of Science, King Saud University, Riyadh 11451, Saudi Arabia*

Complete contact information is available at: https://pubs.acs.org/10.1021/acsomega.3c07596

Author Contributions

#F.R. and I.S. contributed equally.

Notes

The authors declare no competing financial interest.

■ ACKNOWLEDGMENTS

K.C. acknowledges the support from the doctoral research fund of the Affiliated Hospital of Southwest Medical University. The authors extend their appreciation to the Researchers Supporting Project number (RSP2024R253), King Saud University, Riyadh, Saudi Arabia.

■ REFERENCES

(1) Khalid, M.; Ali, A.; Jawaria, R.; Asghar, M. A.; Asim, S.; Khan, M. U.; Hussain, R.; Fayyaz ur Rehman, M.; Ennis, C. J.; Akram, M. S. First Principles Study of Electronic and Nonlinear Optical Properties of A-D-π-A and D-A-D-π-A Configured Compounds Containing Novel Quinoline-Carbazole Derivatives. *RSC Adv.* **2020**, *10* (37), 22273−22283.

(2) Ghiasuddin; Akram, M.; Adeel, M.; Khalid, M.; Tahir, M. N.; Khan, M. U.; Asghar, M. A.; Ullah, M. A.; Iqbal, M. A Combined Experimental and Computational Study of 3-Bromo-5-(2,5-Difluorophenyl) Pyridine and 3,5-Bis(Naphthalen-1-Yl)Pyridine: Insight into the Synthesis, Spectroscopic, Single Crystal XRD, Electronic, Nonlinear Optical and Biological Properties. *J. Mol. Struct.* **2018**, *1160*, 129−141.

(3) Shahid, M.; Salim, M.; Khalid, M.; Tahir, M. N.; Khan, M. U.; Braga, A. A. C. Synthetic, XRD, Non-Covalent Interactions and Solvent Dependent Nonlinear Optical Studies of Sulfadiazine-Ortho-Vanillin Schiff Base: (E)-4-((2-Hydroxy-3-Methoxy- Benzylidene) Amino)-N-(Pyrimidin-2-Yl)Benzene-Sulfonamide. *J. Mol. Struct.* **2018**, *1161*, 66−75.

(4) Khan, M. U.; Khalid, M.; Shafiq, I.; Khera, R. A.; Shafiq, Z.; Jawaria, R.; Shafiq, M.; Alam, M. M.; Braga, A. A. C.; Imran, M.; Kanwal, F.; Xu, Z.; Lu, C. Theoretical Investigation of Nonlinear Optical Behavior for Rod and T-Shaped Phenothiazine Based D-π-A Organic Compounds and Their Derivatives. *Journal of Saudi Chemical Society* **2021**, *25* (10), No. 101339.

(5) Eaton, D. F. Nonlinear. *Optical Materials.* **1991**, *455*, 128−156.

(6) Khalid, M.; Arshad, M. N.; Murtaza, S.; Shafiq, I.; Haroon, M.; Asiri, A. M.; Figueirêdo de AlcântaraMorais, S.; Braga, A. A. C. Enriching NLO Efficacy via Designing Non-Fullerene Molecules with the Modification of Acceptor Moieties into ICIF2F: An Emerging Theoretical Approach. *RSC Adv.* **2022**, *12* (21), 13412−13427.

(7) Zafar, F.; Mehboob, M. Y.; Hussain, R.; Khan, M. A. U.; Hussain, A.; Hassan, T.; Rashid, M.; Shahi, M. N. End-Capped Engineering of Truxene Core Based Acceptor Materials for High Performance Organic Solar Cells: Theoretical Understanding and Prediction. *Opt. Quantum Electron.* **2021**, *53*, 99.

(8) Khalid, M.; Lodhi, H. M.; Khan, M. U.; Imran, M. Structural Parameter-Modulated Nonlinear Optical Amplitude of Acceptor-π-D-π-Donor-Configured Pyrene Derivatives: A DFT Approach. *RSC Adv.* **2021**, *11* (23), 14237−14250.

(9) Khalid, M.; Ali, A.; Rehman, M. F. U.; Mustaqeem, M.; Ali, S.; Khan, M. U.; Asim, S.; Ahmad, N.; Saleem, M. Exploration of Noncovalent Interactions, Chemical Reactivity, and Nonlinear Optical Properties of Piperidone Derivatives: A Concise Theoretical Approach. *ACS Omega* **2020**, *5* (22), 13236−13249.

(10) Ivanova, B. B.; Spiteller, M. Possible Application of the Organic Barbiturates as NLO Materials. *Cryst. Growth Des* **2010**, *10* (6), 2470−2474.

(11) Knill, E.; Laflamme, R.; Milburn, G. J. A Scheme for Efficient Quantum Computation with Linear Optics. *Nature* **2001**, *409* (6816), 46−52.

(12) Feng, J. D.; Yan, L. K.; Su, Z. M.; Kan, Y. H.; Lan, Y. Q.; Liao, Y.; Zhu, Y. L. Theoretical Studies on Electronic Spectra and Second-Order Nonlinear Optical Properties of Glucosyl Substituted Barbituric Acid Derivatives. *Chin. J. Chem.* **2006**, *24* (1), 119−123.

(13) Khan, I.; Khalid, M.; Adeel, M.; Niaz, S. I.; Shafiq, I.; Muhammad, S.; Braga, A. A. C. Palladium-Catalyzed Synthesis of 5-(Arylated) Pyrimidines, Their Characterization, Electronic Communication, and Non-Linear Optical Evaluations. *J. Mol. Struct.* **2021**, *1237*, No. 130408.

(14) Asokan, P.; Kalainathan, S. Bulk Crystal Growth, Optical, Electrical, Thermal, and Third Order NLO Properties of 2-[4-(Diethylamino)Benzylidene]Malononitrile (DEBM) Single Crystal. *J. Phys. Chem. C* **2017**, *121* (40), 22384−22395.

(15) Jerca, F. A.; Jerca, V. V.; Kajzar, F.; Manea, A. M.; Rau, I.; Vuluga, D. M. Simultaneous Two and Three Photon Resonant Enhancement of Third-Order NLO Susceptibility in an Azo-Dye Functionalized Polymer Film. *Phys. Chem. Chem. Phys.* **2013**, *15* (19), 7060−7063.

(16) Bhattacharya, S.; Biswas, C.; Raavi, S. S. K.; Venkata Suman Krishna, J.; Vamsi Krishna, N.; Giribabu, L.; Soma, V. R. Synthesis, Optical, Electrochemical, DFT Studies, NLO Properties, and Ultrafast Excited State Dynamics of Carbazole-Induced Phthalocyanine Derivatives. *J. Phys. Chem. C* **2019**, *123* (17), 11118−11133.

(17) Janjua, M. R. S. A. Computational Study on Non-Linear Optical and Absorption Properties of Benzothiazole Based Dyes: Tunable Electron-Withdrawing Strength and Reverse Polarity. *Open Chem.* **2017**, *15* (1), 139−146.

(18) Khan, M. U.; Hussain, S.; Asghar, M. A.; Munawar, K. S.; Khera, R. A.; Imran, M.; Ibrahim, M. M.; Hessien, M. M.; Mersal, G. A. M. Exploration of Nonlinear Optical Properties for the First Theoretical Framework of Non-Fullerene DTS(FBTTh 2) 2 -Based Derivatives. *ACS Omega* **2022**, *7* (21), 18027−18040.

(19) Khalid, M.; Khan, M. U.; Shafiq, I.; Hussain, R.; Ali, A.; Imran, M.; Braga, A. A. C.; ur Rehman, M. F.; Akram, S. Structural Modulation of π-Conjugated Linkers in D−π−A Dyes Based on Triphenylamine Dicyanovinylene Framework to Explore the NLO Properties. *R. Soc. Open Sci.* **2021**, *8* (8), No. 210570.

(20) Hou, H.; Song, Y.; Fan, Y.; Zhang, L.; Du, C.; Zhu, Y. A Novel Coordination Polymer [Co(NCS)2(Bpms)2]n (Bpms = 1,2-Bis(4-Pyridylmethyl)Disulfenyl): Synthesis, Crystal Structure and Third-

Order Nonlinear Optical Properties. *Inorg. Chim. Acta* **2001**, *316* (1−2), 140−144.
(21) Jia, J.; Li, T.; Cui, Y.; Li, Y.; Wang, W.; Han, L.; Li, Y.; Gao, J. Study on the Synthesis and Third-Order Nonlinear Optical Properties of D-A Poly-Quinacridone Optical Materials. *Dyes Pigm.* **2019**, *162*, 26−35.
(22) Fuks-Janczarek, I.; Luc, J.; Sahraoui, B.; Dumur, F.; Hudhomme, P.; Berdowski, J.; Kityk, I. V. Third-Order Nonlinear Optical Figure of Merits for Conjugated TTF-Quinone Molecules. *J. Phys. Chem. B* **2005**, *109*, 10179−10183.
(23) Biswal, B. P.; Valligatla, S.; Wang, M.; Banerjee, T.; Saad, N. A.; Mariserla, B. M. K.; Chandrasekhar, N.; Becker, D.; Addicoat, M.; Senkovska, I.; Berger, R.; Rao, D. N.; Kaskel, S.; Feng, X. Nonlinear Optical Switching in Regioregular Porphyrin Covalent Organic Frameworks. *Angew. Chem.* **2019**, *131* (21), 6970−6974.
(24) Chen, B.; Ni, S.; Sun, L.; Luo, X.; Zhang, Q.; Song, Y.; Zhong, Q.; Fang, Y.; Huang, C.; Chen, S.; Wu, W. Intramolecular Charge Transfer Tuning of Azo Dyes: Spectroscopic Characteristic and Third-Order Nonlinear Optical Properties. *Dyes Pigm.* **2018**, *158*, 474−481.
(25) Wielopolski, M.; Kim, J. H.; Jung, Y. S.; Yu, Y. J.; Kay, K. Y.; Holcombe, T. W.; Zakeeruddin, S. M.; Grätzel, M.; Moser, J. E. Position-Dependent Extension of π-Conjugation in D-π-A Dye Sensitizers and the Impact on the Charge-Transfer Properties. *J. Phys. Chem. C* **2013**, *117*, 13805−13815.
(26) Katono, M.; Wielopolski, M.; Marszalek, M.; Bessho, T.; Moser, J. E.; Humphry-Baker, R.; Zakeeruddin, S. M.; Grätzel, M. Effect of Extended π-Conjugation of the Donor Structure of Organic D-A-π-A Dyes on the Photovoltaic Performance of Dye-Sensitized Solar Cells. *J. Phys. Chem. C* **2014**, *118*, 16486−16493.
(27) Panneerselvam, M.; Kathiravan, A.; Solomon, R. V.; Jaccob, M. The Role of π-Linkers in Tuning the Optoelectronic Properties of Triphenylamine Derivatives for Solar Cell Applications - A DFT/TDDFT Study. *Phys. Chem. Chem. Phys.* **2017**, *19*, 6153−6163.
(28) Nalwa, H. S. Organic Materials for Third-Order Nonlinear Optics. *Adv. Mater.* **1993**, *5* (5), 341−358.
(29) Pinna, A.; Malfatti, L.; Piccinini, M.; Falcaro, P.; Innocenzi, P. Hybrid Materials with an Increased Resistance to Hard X-Rays Using Fullerenes as Radical Sponges. *J. Synchrotron Radiat* **2012**, *19* (4), 586−590.
(30) Guldi, D. M.; Illescas, B. M.; Atienza, C. M.; Wielopolski, M.; Martín, N. Fullerene for Organic Electronics. *Chem. Soc. Rev.* **2009**, *38* (6), 1587−1597.
(31) Couris, S.; Koudoumas, E.; Ruthf, A. A.; Leacht, S. Concentration and Wavelength Dependence of the Effective Third-Order Susceptibility and Optical Limiting of Ceo in Toluene Solution. *J. Phys. B: At., Mol. Opt. Phys.* **1995**, *28* (20), 4537−4554.
(32) Ye, Q. Q.; Wang, Z. K.; Li, M.; Zhang, C. C.; Hu, K. H.; Liao, L. S. N-Type Doping of Fullerenes for Planar Perovskite Solar Cells. *ACS Energy Lett.* **2018**, *3* (4), 875−882.
(33) Dai, S.; Xiao, Y.; Xue, P.; James Rech, J.; Liu, K.; Li, Z.; Lu, X.; You, W.; Zhan, X. Effect of Core Size on Performance of Fused-Ring Electron Acceptors. *Chem. Mater.* **2018**, *30* (15), 5390−5396.
(34) Zhan, C.; Zhang, X.; Yao, J. New Advances in Non-Fullerene Acceptor Based Organic Solar Cells. *RSC Adv.* **2015**, *5* (113), 93002−93026.
(35) Khalid, M.; Khan, M. U.; Hussain, R.; Irshad, S.; Ali, B.; Braga, A. A. C.; Imran, M.; Hussain, A. Exploration of Second and Third Order Nonlinear Optical Properties for Theoretical Framework of Organic D−π−D−π−A Type Compounds. *Opt. Quantum Electron.* **2021**, *53* (10), 561 DOI: 10.1007/s11082-021-03212-3.
(36) Khalid, M.; Hussain, R.; Hussain, A.; Ali, B.; Jaleel, F.; Imran, M.; Assiri, M. A.; Khan, M. U.; Ahmed, S.; Abid, S.; Haq, S.; Saleem, K.; Majeed, S.; Tariq, C. J.; Palafox, M. A. Electron Donor and Acceptor Influence on the Nonlinear Optical Response of Diacetylene-Functionalized Organic Materials (DFOMs): Density Functional Theory. *Molecules* **2019**, *24*, 2096.
(37) Khalid, M.; Zafar, M.; Hussain, S.; Asghar, M. A.; Khera, R. A.; Imran, M.; Abookleesh, F. L.; Akram, M. Y.; Ullah, A. Influence of End-Capped Modifications in the Nonlinear Optical Amplitude of Nonfullerene-Based Chromophores with a D-π-A Architecture: A DFT/TDDFT Study. *ACS Omega* **2022**, *7* (27), 23532−23548.
(38) Gong, P.; An, L.; Tong, J.; Liu, X.; Liang, Z.; Li, J. Design of A-D-A-Type Organic Third-Order Nonlinear Optical Materials Based on Benzodithiophene: A DFT Study. *Nanomaterials* **2022**, *12* (20), 3700.
(39) Gobbi, L.; Elmaci, N.; Lüthi, H. P. N,N-Dialkylaniline-Substituted Tetraethynylethenes: A New Class of Chromophores Possessing an Emitting Charge-Transfer State. Experimental and Computational Studies. *ChemPhysChem* **2001**, *2*, 423.
(40) Mehboob, M. Y.; Hussain, R.; Irshad, Z.; Adnan, M. Enhancement in the Photovoltaic Properties of Hole Transport Materials by End-Capped Donor Modifications for Solar Cell Applications. *Bull. Korean Chem. Soc.* **2021**, *42* (4), 597−610.
(41) Zhang, D.; Xu, P.; Wu, T.; Ou, Y.; Yang, X.; Sun, A.; Cui, B.; Sun, H.; Hua, Y. Cyclopenta[Hi]Aceanthrylene-Based Dopant-Free Hole-Transport Material for Organic−Inorganic Hybrid and All-Inorganic Perovskite Solar Cells. *J. Mater. Chem. A Mater.* **2019**, *7* (10), 5221−5226.
(42) Lu, B.; Xiao, Y.; Li, T.; Liu, K.; Lu, X.; Lian, J.; Zeng, P.; Qu, J.; Zhan, X. Z-Shaped Fused-Chrysene Electron Acceptors for Organic Photovoltaics. *ACS Appl. Mater. Interfaces* **2019**, *11* (36), 33006−33011.
(43) Uzun, S.; Esen, Z.; Koç, E.; Usta, N. C.; Ceylan, M. Experimental and Density Functional Theory (MEP, FMO, NLO, Fukui Functions) and Antibacterial Activity Studies on 2-Amino-4-(4-Nitrophenyl) −5,6-Dihydrobenzo [h] Quinoline-3-Carbonitrile. *J. Mol. Struct.* **2019**, *1178*, 450−457.
(44) Khalid, M.; Shafiq, I.; Zhu, M.; Khan, M. U.; Shafiq, Z.; Iqbal, J.; Alam, M. M.; Braga, A. A. C.; Imran, M. Efficient Tuning of Small Acceptor Chromophores with A1-π-A2-π-A1 Configuration for High Efficacy of Organic Solar Cells via End Group Manipulation. *Journal of Saudi Chemical Society* **2021**, *25* (8), No. 101305.
(45) Shafiq, I.; Khalid, M.; Asghar, M. A.; Adeel, M.; Fayyaz ur Rehman, M.; Syed, A.; Bahkali, A. H.; Elgorban, A. M.; Akram, M. S. Exploration of Photovoltaic Behavior of Benzodithiophene Based Non-Fullerene Chromophores: First Theoretical Framework for Highly Efficient Photovoltaic Parameters. *J. Mater. Res. Technol.* **2023**, *24*, 1882.
(46) Khalid, M.; Khan, M. U.; Shafiq, I.; Hussain, R.; Mahmood, K.; Hussain, A.; Jawaria, R.; Hussain, A.; Imran, M.; Assiri, M. A.; Ali, A.; ur Rehman, M. F.; Sun, K.; Li, Y., NLO Potential Exploration for D−π−A Heterocyclic Organic Compounds by Incorporation of Various π-Linkers and Acceptor Units. *Arabian J. Chem.* 2021 *14* 103295 Elsevier DOI: 10.1016/j.arabjc.2021.103295.
(47) Janjua, M. R. S. A. Prediction and Understanding: Quantum Chemical Framework of Transition Metals Enclosed in a B12N12Inorganic Nanocluster for Adsorption and Removal of DDT from the Environment. *Inorg. Chem.* **2021**, *60* (14), 10837−10847.
(48) Pearson, R. G. Absolute Electronegativity and Hardness Correlated with Molecular Orbital Theory. *Proc. Natl. Acad. Sci. U. S. A.* **1986**, *83* (22), 8440−8441.
(49) Khalid, M.; Ali, M.; Aslam, M.; Sumrra, S. H.; Khan, M. U.; Raza, N.; Kumar, N.; Imran, M. Frontier Molecular, Natural Bond Orbital, Uv-Vis Spectral Study, Solvent Influence on Geometric Parameters, Vibrational Frequencies and Solvation Energies of 8-Hydroxyquinoline. *Int. J. Pharm. Sci. Res.* **2017**, *8* (2), 457.
(50) Siddiqui, W. A.; Khalid, M.; Ashraf, A.; Shafiq, I.; Parvez, M.; Imran, M.; Irfan, A.; Hanif, M.; Khan, M. U.; Sher, F.; Ali, A. Antibacterial Metal Complexes of O-Sulfamoylbenzoic Acid: Synthesis, Characterization, and DFT Study. *Appl. Organomet. Chem.* **2022**, *36* (1), No. e6464.
(51) Cremer, J.; Briehn, C. A. Novel Highly Fluorescent Triphenylamine-Based Oligothiophenes. *Chem. Mater.* **2007**, *19* (17), 4155−4165.
(52) Mitschke, U.; Bäuerle, P. The Electroluminescence of Organic Materials. *J. Mater. Chem.* **2000**, *10* (7), 1471−1507.

https://doi.org/10.1021/acsomega.3c07596
ACS Omega 2024, 9, 3596−3608

(53) Dimitrakopoulos, C. D.; Malenfant, P. R. L. Organic Thin Film Transistors for Large Area Electronics. *Adv. Mater.* **2002**, *14* (2), 99−117.
(54) Satoh, N.; Nakashima, T.; Yamamoto, K. Metal-Assembling Dendrimers with a Triarylamine Core and Their Application to a Dye-Sensitized Solar Cell. *J. Am. Chem. Soc.* **2005**, *127* (37), 13030−13038.
(55) Wang, Q.; Zakeeruddin, S. M.; Cremer, J.; Bäuerle, P.; Humphry-Baker, R.; Grätzel, M. Cross Surface Ambipolar Charge Percolation in Molecular Triads on Mesoscopic Oxide Films. *J. Am. Chem. Soc.* **2005**, *127* (15), 5706−5713.
(56) Kong, L.; Yang, J.; Zhou, H.; Li, S.; Hao, F.; Zhang, Q.; Tu, Y.; Wu, J.; Xue, Z.; Tian, Y. Synthesis, Photophysical Properties and TD-DFT Calculation of Four Two-Photon Absorbing Triphenylamine Derivatives. *Sci. China Chem.* **2013**, *56* (1), 106−116.
(57) Yang, Y.; Liu, F.; Wang, H.; Bo, S.; Liu, J.; Qiu, L.; Zhen, Z.; Liu, X. Enhanced Electro-Optic Activity from the Triarylaminophenyl-Based Chromophores by Introducing Heteroatoms to the Donor. *J. Mater. Chem. C Mater.* **2015**, *3* (20), 5297−5306.
(58) Janjua, M. R. S. A. First Theoretical Framework of Di-Substituted Donor Moieties of Triphenylamine and Carbazole for NLO Properties: Quantum Paradigms of Interactive Molecular Computation. *Mol. Simul* **2017**, *43* (18), 1539−1545.
(59) El-Zohry, A. M.; Roca-Sanjuán, D.; Zietz, B. Ultrafast Twisting of the Indoline Donor Unit Utilized in Solar Cell Dyes: Experimental and Theoretical Studies. *J. Phys. Chem. C* **2015**, *119* (5), 2249−2259.
(60) Fakis, M.; Stathatos, E.; Tsigaridas, G.; Giannetas, V.; Persephonis, P. Femtosecond Decay and Electron Transfer Dynamics of the Organic Sensitizer D149 and Photovoltaic Performance in Quasi-Solid-State Dye-Sensitized Solar Cells. *J. Phys. Chem. C* **2011**, *115* (27), 13429−13437.
(61) Yang, J.; Ganesan, P.; Teuscher, J.; Moehl, T.; Kim, Y. J.; Yi, C.; Comte, P.; Pei, K.; Holcombe, T. W.; Nazeeruddin, M. K.; Hua, J.; Zakeeruddin, S. M.; Tian, H.; Grätzel, M. Influence of the Donor Size in D-π-A Organic Dyes for Dye-Sensitized Solar Cells. *J. Am. Chem. Soc.* **2014**, *136* (15), 5722−5730.
(62) Chang, C.; Kuo, I.; Lin, J.; Lu, Y.; Chen, C.; Back, H.; Lou, P.; Chang, T. A Novel Carbazole Derivative, BMVC: A Potential Antitumor Agent and Fluorescence Marker of Cancer Cells. *Chem. Biodiversity* **2004**, *1* (9), 1377−1384.
(63) Teng, C.; Yang, X.; Yuan, C.; Li, C.; Chen, R.; Tian, H.; Li, S.; Hagfeldt, A.; Sun, L. Two Novel Carbazole Dyes for Dye-Sensitized Solar Cells with Open-Circuit Voltages up to 1 v Based on Br-/Br3- Electrolytes. *Org. Lett.* **2009**, *11* (23), 5542−5545.
(64) Sudyoadsuk, T.; Pansay, S.; Morada, S.; Rattanawan, R.; Namuangruk, S.; Kaewin, T.; Jungsuttiwong, S.; Promarak, V. Synthesis and Characterization of D-D-π-A-Type Organic Dyes Bearing Carbazole-Carbazole as a Donor Moiety (D-D) for Efficient Dye-Sensitized Solar Cells. *Eur. J. Org. Chem.* **2013**, *2013*, 5051−5063.
(65) Bloor, J. E.; Gilson, B. R.; Haas, R. J.; Zirkle, C. L. Electron-Donating Properties of Phenothiazine and Related Compounds. *J. Med. Chem.* **1970**, *13* (5), 922−925.
(66) Liu, F.; Wang, H.; Yang, Y.; Xu, H.; Yang, D.; Bo, S.; Liu, J.; Zhen, Z.; Liu, X.; Qiu, L. Using Phenoxazine and Phenothiazine as Electron Donors for Second-Order Nonlinear Optical Chromophore: Enhanced Electro-Optic Activity. *Dyes Pigm.* **2015**, *114* (C), 196−203.
(67) Arshad, M. N.; Khalid, M.; Asad, M.; Braga, A. A. C.; Asiri, A. M.; Alotaibi, M. M. Influence of Peripheral Modification of Electron Acceptors in Nonfullerene (O-IDTBR1)-Based Derivatives on Nonlinear Optical Response: DFT/TDDFT Study. *ACS Omega* **2022**, *7* (14), 11631−11642.
(68) Khalid, M.; Khan, M. U.; Azhar, N.; Arshad, M. N.; Asiri, A. M.; Braga, A. A. C.; Akhtar, M. N. Exploration of Nonlinear Optical Enhancement and Interesting Optical Behavior with Pyrene Moiety as the Conjugated Donor and Efficient Modification in Acceptor Moieties. *Opt. Quantum Electron.* **2022**, *54* (7), 395.
(69) Arshad, M. N.; Khalid, M.; Shabbir, Ghulam; Asad, M.; Asiri, A. M.; Alotaibi, M. M.; Braga, A. A. C.; Khan, A. Donor Moieties with D-π-a Framing Modulated Electronic and Nonlinear Optical Properties for Non-Fullerene-Based Chromophores. *RSC Adv.* **2022**, *12* (7), 4209−4223.
(70) Tariq, S.; Khalid, M.; Raza, A. R.; Rubab, S. L.; Morais, S. F. D. A.; Khan, M. U.; Tahir, M. N.; Braga, A. A. C. Experimental and Computational Investigations of New Indole Derivatives: A Combined Spectroscopic, SC-XRD, DFT/TD-DFT and QTAIM Analysis. *J. Mol. Struct.* **2020**, *1207*, No. 127803.
(71) Pasha, A. R.; Khalid, M.; Shafiq, Z.; Khan, M. U.; Naseer, M. M.; Tahir, M. N.; Hussain, R.; Braga, A. A. C.; Jawaria, R. A Comprehensive Study of Structural, Non-Covalent Interactions and Electronic Insights into N-Aryl Substituted Thiosemicarbazones via SC-XRD and First-Principles DFT Approach. *J. Mol. Struct.* **2021**, *1230*, No. 129852.
(72) WEINHOLD, F.; LANDIS, C. R. Natural Bond Orbitals and Extensions of Localized Bonding Concepts. *Chem. Educ. Res. Pract.* **2001**, *2* (2), 91−104.
(73) Khalid, M.; Ali, A.; De la Torre, A. F.; Marrugo, K. P.; Concepcion, O.; Kamal, G. M.; Muhammad, S.; Al-Sehemi, A. G. Facile Synthesis, Spectral (IR, Mass, UV−Vis, NMR), Linear and Nonlinear Investigation of the Novel Phosphonate Compounds: A Combined Experimental and Simulation Study. *ChemistrySelect* **2020**, *5* (10), 2994−3006.
(74) Khalid, M.; Ali, A.; Khan, M. U.; Tahir, M. N.; Ahmad, A.; Ashfaq, M.; Hussain, R.; Morais, S. F. d. A.; Braga, A. A. C. Non-Covalent Interactions Abetted Supramolecular Arrangements of N-Substituted Benzylidene Acetohydrazide to Direct Its Solid-State Network. *J. Mol. Struct.* **2021**, *1230*, No. 129827.
(75) Gokula Krishnan, K.; Sivakumar, R.; Thanikachalam, V.; Saleem, H.; Arockia Doss, M. Synthesis, Spectroscopic Investigation and Computational Study of 3-(1-(((Methoxycarbonyl)Oxy)Imino)-Ethyl)-2H-Chromen-2-One. *Spectrochim Acta A Mol. Biomol Spectrosc* **2015**, *144*, 29−42.
(76) Glendening, E. D.; Landis, C. R.; Weinhold, F. Natural Bond Orbital Methods. *Wiley Interdiscip Rev. Comput. Mol. Sci.* **2012**, *2* (1), 1−42.
(77) Lee, J.; Lee, S. M.; Chen, S.; Kumari, T.; Kang, S. H.; Cho, Y.; Yang, C. Organic Photovoltaics with Multiple Donor−Acceptor Pairs. *Adv. Mater.* **2019**, *31* (20), No. 1804762, DOI: 10.1002/adma.201804762.
(78) Sharif, A.; Jabeen, S.; Iqbal, S.; Iqbal, J. Tuning the Optoelectronic Properties of Dibenzochrysene (DBC) Based Small Molecules for Organic Astral Cells. *Mater. Sci. Semicond. Process.* **2021**, *127*, No. 105689.
(79) Köse, M. E. Evaluation of Acceptor Strength in Thiophene Coupled Donor−Acceptor Chromophores for Optimal Design of Organic Photovoltaic Materials. *J. Phys. Chem. A* **2012**, *116* (51), 12503−12509.
(80) Goszczycki, P.; Stadnicka, K.; Brela, M. Z.; Grolik, J.; Ostrowska, K. Synthesis, Crystal Structures, and Optical Properties of the π-π Interacting Pyrrolo[2,3-b]Quinoxaline Derivatives Containing 2-Thienyl Substituent. *J. Mol. Struct.* **2017**, *1146*, 337−346.
(81) Muhammad, S.; Xu, H.; Su, Z.; Fukuda, K.; Kishi, R.; Shigeta, Y.; Nakano, M. A New Type of Organic-Inorganic Hybrid NLO-Phore with Large off-Diagonal First Hyperpolarizability Tensors: A Two-Dimensional Approach. *Dalton Trans.* **2013**, *42*, 15053−15062.
(82) Muhammad, S.; Al-Sehemi, A. G.; Su, Z.; Xu, H.; Irfan, A.; Chaudhry, A. R. First Principles Study for the Key Electronic, Optical and Nonlinear Optical Properties of Novel Donor-Acceptor Chalcones. *J. Mol. Graph Model* **2017**, *72*, 58−69.
(83) Sheela, N. R.; Muthu, S.; Sampathkrishnan, S. Molecular Orbital Studies (Hardness, Chemical Potential and Electrophilicity), Vibrational Investigation and Theoretical NBO Analysis of 4−4′-(1H-1,2,4-Triazol-1-Yl Methylene) Dibenzonitrile Based on Abinitio and DFT Methods. *Spectrochim Acta A Mol. Biomol Spectrosc* **2014**, *120*, 237−251.

https://doi.org/10.1021/acsomega.3c07596
ACS Omega 2024, 9, 3596−3608

(84) Shafiq, I.; Amanat, I.; Khalid, M.; Asghar, M. A.; Baby, R.; Ahmed, S.; Alshehri, S. M. Influence of Azo-Based Donor Modifications on Nonlinear Optical Amplitude of D-π-A Based Organic Chromophores: A DFT/TD-DFT Exploration. *Synth. Met.* **2023**, *297*, No. 117410.
(85) Muhammad, S.; Shehzad, R. A.; Iqbal, J.; Al-Sehemi, A. G.; Saravanabhavan, M.; Khalid, M. Benchmark Study of the Linear and Nonlinear Optical Polarizabilities in Proto-Type NLO Molecule of Para-Nitroaniline. *J. Theor Comput. Chem.* **2019**, *18* (06), No. 1950030.
(86) Khalid, M.; Shafiq, I.; Umm-e-Hani; Mahmood, K.; Hussain, R.; ur Rehman, M. F.; Assiri, M. A.; Imran, M.; Akram, M. S. Effect of Different End-Capped Donor Moieties on Non-Fullerenes Based Non-Covalently Fused-Ring Derivatives for Achieving High-Performance NLO Properties. *Sci. Rep* **2023**, *13* (1), 1395.
(87) Frisch, M. J.; Clemente, V.; Barone, V.; Mennucci, B.; Petersson, G. A.; Nakatsuji, H.; Caricato, M.; Li, X.; Hratchian, H. P.; Izmaylov, A. F.; Bloino, J.; Zheng, G.; Sonnenberg, J. L.; Frisch, M. J.; Trucks, G.; Schlegel, H. B.; Scuseria, G. E.; Robb, M. A.; Cheeseman, J. R., *Gaussian 09, Revision a. 01*, 2009, 20−44 Gaussian Inc..
(88) Khan, M. U.; Hussain, R.; Mehboob, M. Y.; Khalid, M.; Ehsan, M. A.; Rehman, A.; Janjua, M. R. S. A., First Theoretical Framework of Z-Shaped Acceptor Materials with Fused-Chrysene Core for High Performance Organic Solar Cells *Spectrochim. Acta Part A* 2021 *245* 118938. Elsevier DOI: 10.1016/j.saa.2020.118938.
(89) Choe, J.-I. MPW1PW91 Calculated Structures and IR Spectra of Thiacalix [4] Biscrown-5 Complexed with Alkali Metal Ions. *Bull. Korean Chem. Soc.* **2011**, *32* (5), 1685−1691.
(90) Andersson, M. P.; Uvdal, P. New Scale Factors for Harmonic Vibrational Frequencies Using the B3LYP Density Functional Method with the Triple-ζ Basis Set 6-31+G(d,p). *J. Phys. Chem. A.* **2005**, *109* (12), 2937−2941.
(91) Dennington, R. D.; Keith, T. A.; Millam, J. M. *GaussView 5.0*; Gaussian Inc.: Wallingford, 2008, *20*.
(92) Hanwell, M. D.; Curtis, D. E.; Lonie, D. C.; Vandermeersch, T.; Zurek, E.; Hutchison, G. R. Avogadro: An Advanced Semantic Chemical Editor, Visualization, and Analysis Platform. *J. Cheminform* **2012**, *4* (1), 17.
(93) Zhurko, G. A.; Zhurko, D. A. http://www.chemcraftprog.com. *ChemCraft*, Version 1.6. 2009.
(94) Lu, T.; Chen, F. Multiwfn: A Multifunctional Wavefunction Analyzer. *J. J. of computational chemistry.* **2012**, *33* (5), 580−592.
(95) *OriginPro, Version*. OriginLab Corporation: Northampton, MA, USA. 2016.
(96) Atalay, Y.; Avcı, D.; Başoğlu, A. Linear and Non-Linear Optical Properties of Some Donor-Acceptor Oxadiazoles by Ab Initio Hartree-Fock Calculations. *Struct Chem.* **2008**, *19* (2), 239−246.
(97) Plaquet, A.; Guillaume, M.; Champagne, B.; Castet, F.; Ducasse, L.; Pozzo, J. L.; Rodriguez, V. In Silico Optimization of Merocyanine-Spiropyran Compounds as Second-Order Nonlinear Optical Molecular Switches. *Phys. Chem. Chem. Phys.* **2008**, *10* (41), 6223−6232.

https://doi.org/10.1021/acsomega.3c07596
ACS Omega 2024, 9, 3596−3608